# Positive Ion Emission from Excimer Laser Excited MgO Surfaces

J. T. Dickinson, S. C. Langford, and J. J. Shin
*Department of Physics, Washington State University, Pullman, Washington 99164-2814*

D. L. Doering
*Department of Physics, Wesleyan University, Middletown, Connecticut 06459*
(Received 5 January 1994; revised manuscript received 8 April 1994)

We report measurements of the energy and angular distributions of positive ions (principally $Mg^+$) photodesorbed from polished MgO crystals exposed to 248 nm excimer laser radiation. At low laser fluences, kinetic energies of several eV are observed and angular distributions are highly peaked in the direction perpendicular to the surface. We present an electrostatic model involving Coulombic repulsion of positively charged ions repelled by photoionized $F$ centers.

PACS numbers: 79.20.Ds, 61.72.Ji, 61.80.Ba, 78.66.Nk

Laser induced desorption of ions from wide band gap insulators at photon energies less than the band gap energy has been frequently observed but not well understood [1–3]. In magnesium oxide (band gap 7.9 eV), copious ion emission has been detected at very low laser fluences at $\lambda = 248$ nm (5 eV photons); lattice defects have been shown to play an important role in the desorption and ablation of species from the MgO surface [4–11]. Oxygen vacancy defects ($F$ and $F^+$ centers) were shown to be mechanically introduced into the near surface region by cleaving, polishing, and abrading MgO surfaces; these vacancies originate via a dislocation motion mechanism [12]. Thus, although polishing removes gross features of the surface, it produces a high density of point defects in the near surface region; this is demonstrated by intense photoluminescence associated with $F$ centers [3–8]. These defects interact strongly with 248 nm UV laser [13–16] light and promote positive ion desorption below the ablation threshold, principally $Mg^+$, although weaker $Mg^{2+}$, $MgO^+$, and $Mg_2O^+$ emissions are also observed [17]. Here we present evidence that photoionization of $F$ centers plays a decisive role in photodesorption of positive ions from MgO via Coulomb repulsion. This evidence includes direct measurement of photoelectrons from MgO surfaces irradiated with 5 eV photons, of energy distributions of $Mg^+$ (and $Mg^{2+}$) ion emissions showing kinetic energies ranging from 2–20 eV, and of total ion emission angular distributions (IAD) which are strongly peaked about the surface normal ($\pm 2.5°$) and propose a simple model for these emissions.

Measurements were made in two vacuum systems at pressures of $10^{-7}$ and $10^{-9}$ Torr. No differences in emission behavior were observed for the two systems. Samples were cleaved from 99.99% pure single crystal MgO and polished to 0.25 $\mu$m with diamond paste. The samples were exposed to 248 nm radiation at fluences ranging from 0.1 to 1.1 J/cm$^2$ from a Lambda-Physik Lextra200 excimer with a pulse width of 30 ns. These fluences are well below the threshold for ablation (2–3 J/cm$^2$) on polished specimens.

Electron emission was detected with a Channeltron electron multiplier (CEM), Galileo Electro-optics Model 4039 biased at +300 V on the front cone. The CEM was located in a metal cover with the CEM front cone centered 5 mm behind a 1 cm diam hole. This reduced the field penetration in the region between the CEM and MgO sample. Electrons were distinguished from a signal in coincidence with the laser generated by scattered laser light incident on the CEM by time of flight (TOF) over a 10 cm path length. The area under the resulting electron peak (starting at 20 ns after the laser pulse) was taken as the photoelectron yield from the MgO surface. Ion TOF measurements were accomplished with a UTI 100C quadrupole mass spectrometer (QMS) with the ionizer removed. The region between the sample and entrance to the QMS (a distance of 17.8 cm) was field free so that the only perturbation to the direct flight of the ions to the QMS detector (also a Channeltron) was the small radial oscillations in the quadrupole mass filter (a length of 15 cm) which for the ion energies observed have negligible effect on the measured TOF.

The IAD were measured using a double chevron microchannel plate (MCP) with three flat, appropriately biased parallel grids (80 mesh) spaced 1 cm apart and a phosphor screen visual display. The UV laser light was admitted to the sample at a 45° angle to the sample surface through small holes in the grid assembly. The IAD produced on the phosphor screen were recorded photographically with a 35 mm camera mounted outside the vacuum system. Time exposures of 1–10 min at a laser pulse rate of 10 Hz were required to produce the images.

Angular distributions of the emitted ions were determined by comparing patterns on the phosphor screen and ion trajectories through the ion optics performed with the SIMION modeling program [18].

Ion flight trajectories from MgO model clusters were also simulated, where the effects of different defect and adion (a low coordination surface cation) positions and initial and final charge states were probed. The ion trajectories were determined by summing the Coulomb

 0031-9007/94/73(19)/2630(4)$06.00 

force on $Mg^+$ or $Mg^{2+}$ ions positioned atop a surface of a 19 × 19 × 10 array of lattice sites populated by $Mg^{2+}$ and $O^{2-}$ in the rocksalt structure; the adsorbed ion was initially in the center of the 19 × 19 face. Assuming a different ionicity would not affect the trajectories but would change the energy of the emitted ion. The ground state $F$ center was modeled by a $-2e$ charge centered at the lattice site of the oxygen vacancy, the $F^+$ center by a $-e$ charge centered at the lattice site of the oxygen vacancy, and the fully ionized $F^{2+}$ center by a completely empty vacancy. No relaxation of the surrounding ions was included.

Figure 1 shows TOF curves for mass-to-charge ratios of 24 ($Mg^+$) and 12 ($Mg^{2+}$) from polished MgO surfaces irradiated at 1.1 J/cm$^2$. Figure 1(a) is a typical single pulse TOF curve for $Mg^+$; the distribution shows a double peak. Although not as convincing, a double peak is also observed when the TOF data are averaged over several pulses [Fig. 1(b)]. The smearing of the double peak is due to random pulse-to-pulse shifts in peak positions (typically $< \pm 2$ $\mu$s) and relative peak heights. Figure 1(c) shows the $Mg^{2+}$ TOF distribution, averaged over several pulses, showing even more clearly two peaks. To avoid possible alteration of the surface due to repeated pulses, sequences of such TOF spectra were acquired on several spots. The two peak structure was always evident but showed random fluctuations in relative peak heights and peak positions (typically $\pm 3$ $\mu$s). To facilitate numerical analysis, the TOF curves [Figs. 2(b) and 2(c)] were fitted assuming that the energy distribution $n(E)$ could be empirically expressed as a sum of two Gaussians, yielding a TOF distribution of the form

$$I(t) = \frac{md^2}{t^3}\left\{N_1 \exp\left[\frac{-(E_1 - E)^2}{2\sigma_1^2}\right] + N_2 \exp\left[\frac{-(E_2 - E)^2}{2\sigma_2^2}\right]\right\}, \quad (1)$$

where $N_1$, $N_2$, $E_1$, $E_2$, $\sigma_1$, and $\sigma_2$ are model parameters, and $E(t)$ is the ion kinetic energy ($= mv^2/2 = md^2/2t^2$) corresponding to the time of arrival $t$ and flight path distance $d$ (22 cm). Equation (1) provides a very good representation of the data shown in Fig. 1. The four corresponding energy distributions are shown in Fig. 2, all normalized to the same height. The most probable energies are 2 and 7.9 eV for $Mg^+$ and 6.7 and 18 eV for $Mg^{2+}$. The error bars on these numbers are conservatively $\pm 1$ eV. Within this uncertainty, the energy distributions show no shift with laser fluence over a range of 0.1 to 2 J/cm$^2$. These relatively high values of kinetic energy and the substantial shifts to higher energies for $Mg^+$ vs $Mg^{2+}$ strongly suggest an electrostatic ejection mechanism for these emissions triggered by the incident 5 eV photons. We propose that the initial step in this process is the photoionization of $F$ centers as follows:

$$F^0 + h\nu \longrightarrow F^+ + e^-, \quad (2)$$

$$F^+ + h\nu \longrightarrow F^{2+} + e^-. \quad (3)$$

Thus, these two positively charged defects ($F^+, F^{2+}$) serving as repulsive centers, combined with two ionic charges ($Mg^+, Mg^{2+}$) could produce the four observed kinetic energy peaks.

Although photoelectron emission from perfect MgO surfaces with 5 eV incident light cannot occur, surface $F^0$ and $F^+$ centers are stable and are both within reach of

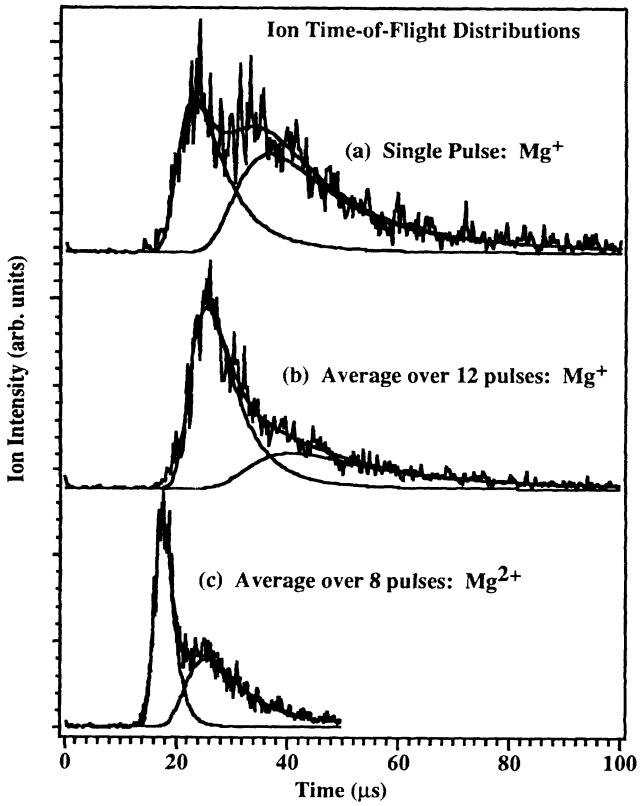


FIG. 1. Mass selected ion time-of-flight distributions for ions desorbed from a polished MgO surface irradiated with 248 nm light at 1.1 J/cm$^2$ per pulse. (a) A single pulse $Mg^+$ TOF curve; (b) average of 12 pulses for $Mg^+$; and (c) average of eight pulses for $Mg^{2+}$. The curve fits shown are from Eq. (1).

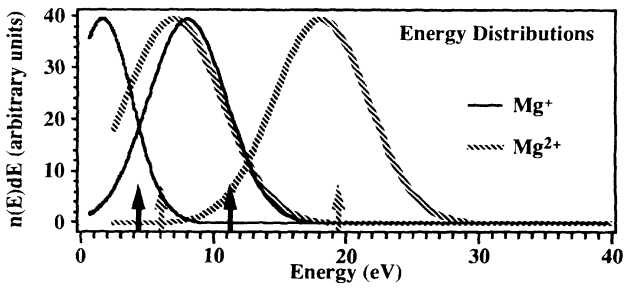


FIG. 2. The energy distributions produced by transforming the four TOF peaks shown in Fig. 1. The distributions have all been normalized to the same height.

vacuum level states [10]. As seen in Fig. 3(a), negative charge emission is observed as a peak (shaded) arriving between ~20–100 ns, which is reasonable for low energy electrons accelerated by the positive voltage applied to the CEM front cone. The relative intensities of the electron emission vs laser fluence are shown in Fig. 3(b), indicating that the emission saturates at low fluence—i.e., all of the surface defects providing electrons are being detected. We conclude that $F$ centers are indeed photoionized, providing strong centers of positive, repulsive charge. Importantly, we also plot in Fig. 3 the fluence dependence of the positive ions (principally $Mg^+$) normalized to the electron data at a single point, showing that positive ion emission tracks the electron emission very closely. Both signals have been detected below our ability to reliably measure fluence ($< 2$ mJ/cm$^2$). Such low fluence emissions plus the shape of these curves (not quadratic) suggest that two photon processes are highly unlikely.

Figure 4(a) shows an IAD image produced by ions originating from a polished single crystal of MgO irradiated at ~400 mJ/cm$^2$ laser fluence. The pattern shows up as a very bright core surrounded by a weak halo. All other features seen here are artifacts due to MCP corona on damaged regions. (Biasing $G_2$ with +100 V repels the desorbed ions and completely removes the bright spot and halo; the artifacts remain.) SIMION modeling of the ion trajectories indicates that the core represents an emission "cone" with a very narrow angular spread of ±2.5°, while the weak halo represents an emission cone of ±13°.

In order to test if extended surface charging was the source of energetic, highly directed positive ions, we also examined the emissions from ~500 nm polycrystalline thin films of oxygen deficient (therefore containing $F$ centers [19]) MgO grown on a silicon (111) substrate

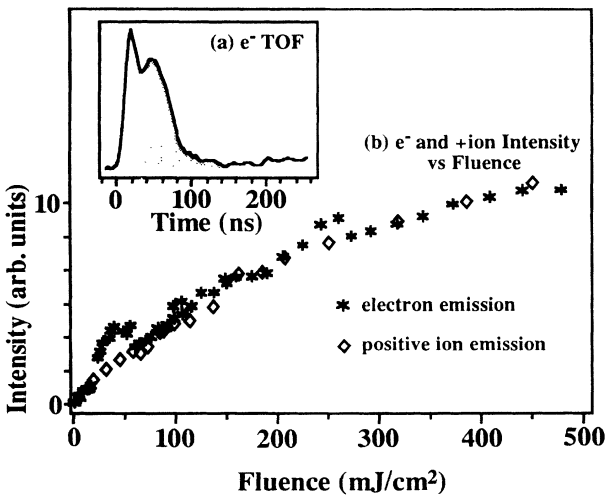


FIG. 3. (a) Fast time-of-flight curve of negative charge detected with a shielded CEM accompanying 248 nm irradiation at 150 mJ/cm$^2$ per pulse; the shaded area represents the photoelectrons emitted from the MgO surface. (b) Intensity of photoelectron and positive ion emissions vs laser fluence.

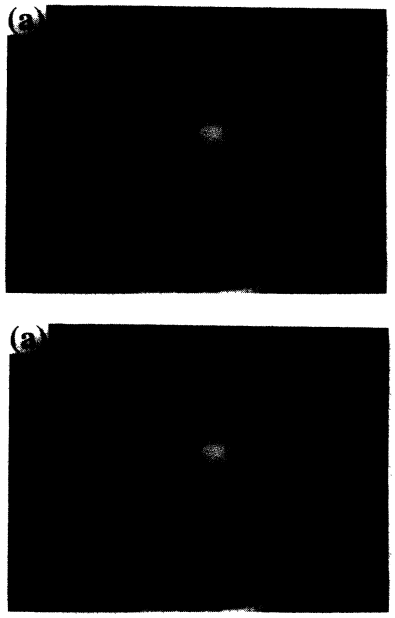


FIG. 4. Photographs of the phosphor screen during laser irradiation of (a) a polished MgO crystal (exposure time, 5 min) and (b) an oxygen deficient MgO thin film (exposure time, 1 min).

by laser ablation in vacuum; charging would be rapidly neutralized through such a thin film. Photoelectrons and copious photodesorbed $Mg^+$ (as well as the other positive ions seen from crystalline MgO) with similar energy distributions were observed at very low laser fluences. The resulting IAD image for such a thin film is shown in Fig. 4(b); it is slightly more diffuse than the polished single crystal, with a core emission cone of ±4° in width and a halo of less than ±15°. The emission from the film appears to have multiple cores, possibly due to its polycrystalline structure. We conclude that the energetic, highly directed positive ions we are observing from single crystal MgO are not caused by surface charging.

Madlung energy calculations [20] were made for the binding energies of adion/$F$ center combinations (one ion and one $F$ center) for a variety of initial and final charge states assuming bulk interionic distances. Ion trajectories from defect-containing clusters for unstable final states were then simulated with the addition of a negative image charge of magnitude $q(\varepsilon - 1)/(\varepsilon + 1)$, where $\varepsilon$ is the MgO dielectric constant and $q$ is the charge on the ion [21]. These calculations indicate that the only final states which unambiguously yield emission accompanying a one or two electron photoemission event (creating a $F^+$ of $F^{2+}$ center) are $Mg^+$ or $Mg^{2+}$ ions adsorbed atop a surface $F$ center. Kinetic energies of adions atop step sites showed comparable (but not larger) values. Calculated final kinetic energies were as follows: a $Mg^+$ above a $F^+$ site, 4.4 eV; $Mg^+$ above a $F^{2+}$ site, 11.2 eV; a $Mg^{2+}$ above a $F^+$ site, 6.0 eV; and a $Mg^{2+}$ above a $F^{2+}$ site, 19.6 eV. These values are shown as arrows along

the energy axis in Fig. 2. Given the simplicity of our point charge electrostatic model, these predictions show reasonable agreement with the measured most probable energies.

It is our opinion that the initial state (before ionization) is a $Mg^{2+}$ adion above a $F^0$ center. Thus, formation of the $Mg^+$ ion would probably involve a photoinduced charge exchange of the form

$$F^0 + Mg^{2+}(\text{adion}) + h\nu \longrightarrow F^+ + Mg^+, \quad (4)$$

possibly resulting in a $Mg^+$ ion located in a lower (but repulsive) potential position than we are assuming (one bulk lattice displacement above the unrelaxed O vacancy). An additional ionization step applied to (4) would generate the $F^{2+}$ repulsive center acting on an $Mg^+$. The continuum of energies seen in Fig. 3 is attributed to the following: (a) near-surface charge exchange which could occur over a range of positions and local potentials, (b) variations in the initial adion position within its binding site, and (c) variations in the distribution of positions and numbers of nearby photoionized vacancies.

Trajectory simulations show that releasing $Mg^+$ or $Mg^{2+}$ ions from directly atop a surface $F^+$ or $F^{2+}$ yields trajectories that are normal to the surface as expected from symmetry. Release of initially stationary adions displaced $\pm 0.23$ Å (maximum of vibrational displacement at 300 K) from the symmetry axis results in only a $\pm 0.2°$ angle spread in the final trajectory. Broadening of the angular distributions due to thermal velocity components parallel to the surface is much greater. Assuming that the adsorbed ion sits in a classical 2D harmonic potential well its time average velocity is ~420 m/s at room temperature. The trajectory of an "average" $Mg^+$ with 7 eV initial electrostatic potential energy would be inclined about $\pm 3.2°$ to the surface normal, in reasonable agreement with the observed width of the central, bright portion of the angular distribution.

The diffuse halos in the IAD extend to considerably larger values ($\pm 12.5°$ for crystalline MgO); we attribute these features to ion trajectories perturbed by one or more additional nearby $F$ centers.

We have demonstrated that photodesorbed positive ion emission, principally $Mg^+$, from MgO surfaces during sub-band-gap 248 nm laser irradiation is energetic, accompanied by photoelectron emission, and highly collimated along the surface normal. Anion vacancy defects are necessary for this emission and are readily introduced mechanically or by control of composition in the case of thin films. Madelung energy estimates and ion trajectory simulations suggest that the most probable emission mechanism is the electrostatic ejection of cations adsorbed atop surface $F$ centers photoionized by the laser. The breadth of the vary sharp inner core of the IAD are consistent with the influence of the thermal velocity component of the adion directed along the surface normal.

The authors wish to thank Les Jensen for assisting in acquiring the IAD images and Mary Dawes for help in the photo laboratory. This work was supported by the Department of Energy under Contract No. DE-FG06-92ER14252, Battelle PNL, and the Washington Technology Center.

[1] E. Matthias, H.B. Nielsen, J. Reif, A. Rosen, and E. Westin, J. Vac. Sci. Technol. B **5**, 1415 (1987).
[2] E. Matthias and T.A. Green, in *Desorption Induced by Electronic Transitions, DIET IV,* edited by G. Betz and P. Varga (Springer-Verlag, Berlin, 1990), pp. 112–127.
[3] L.L. Chase, A.V. Hamza, and H.W. Lee, in *Laser Ablation: Mechanisms and Applications,* edited by J.C. Miller and R.F. Haglund, Jr. (Springer-Verlag, Berlin, 1991), pp. 193–202.
[4] J.T. Dickinson, S.C. Langford, and L.C. Jensen, in *Lasers in Microelectronic Manufacturing,* SPIE Proceedings Vol. 1598 (SPIE-International Society for Optical Engineering, Bellingham, WA, 1991), p. 72.
[5] R.L. Webb, S.C. Langford, L.C. Jensen, and J.T. Dickinson, Mater. Res. Soc. Symp. Proc. **236**, 21 (1992).
[6] R.L. Webb, L.C. Jensen, S.C. Langford, and J.T. Dickinson, J. Appl. Phys. **74**, 2323 (1993).
[7] See Ref. [6], p. 2338.
[8] J.T. Dickinson, L.C. Jensen, R.L. Webb, M.L. Dawes, and S.C. Langford, Proc. Mater. Res. Soc. **285**, 131 (1993).
[9] J.T. Dickinson, L.C. Jensen, R.L. Webb, M.L. Dawes, and S.C. Langford, J. Appl. Phys. **74**, 3758 (1993).
[10] J.T. Dickinson, L.C. Jensen, R.L. Webb, and S.C. Langford, in *Laser Ablation: Mechanisms and Applications-II—1993,* AIP Conf. Proc. No. 288 (AIP, New York, 1993), pp. 13–25.
[11] J.T. Dickinson, L.C. Jensen, R.L. Webb, and S.C. Langford, J. Non-Cryst. Solids (to be published).
[12] J.P. Hirth and J. Lothe, *Theory of Dislocations* (Wiley, New York, 1982), 2nd ed., pp. 602–603.
[13] G.H. Rosenblatt, M.W. Rowe, G.P. Williams, Jr., R.T. Williams, and Y. Chen, Phys. Rev. B **39**, 10309 (1989).
[14] A. Gibson, R. Haydock, and J.P. LeFemina, Appl. Surf. Sci. **72**, 285 (1993).
[15] A. Gibson, R. Haydock, and J.P. LeFemina, Phys. Rev. B **50**, 2582 (1994).
[16] L.A. Kappers, R.L. Kroes, and E.B. Hensley, Phys. Rev. B **1**, 4151 (1970).
[17] J.J. Shin and J.T. Dickinson, "Photodesorption of Positive Ions from MgO" (to be published).
[18] D.A. Dahl and J.E. Delmore, EG&G Idaho Report No. EGG-CS-7233, 1988.
[19] Ming-Cheng Wu, C.M. Truong, and D.W. Goodman, **46**, 12688 (1992).
[20] J. Magill, J. Bloem, and R.W. Ohse, J. Chem. Phys. **76**, 6227 (1982).
[21] J.D. Jackson, *Classical Electrodynamics* (Wiley, New York, 1975), 2nd ed., p. 148.

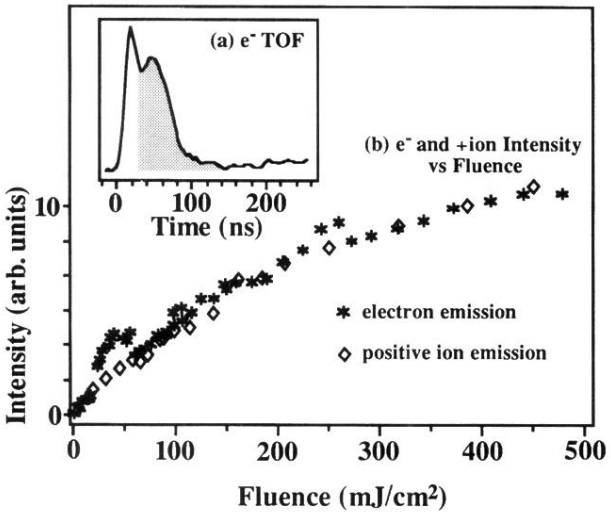


FIG. 3. (a) Fast time-of-flight curve of negative charge detected with a shielded CEM accompanying 248 nm irradiation at 150 $mJ/cm^2$ per pulse; the shaded area represents the photoelectrons emitted from the MgO surface. (b) Intensity of photoelectron and positive ion emissions vs laser fluence.

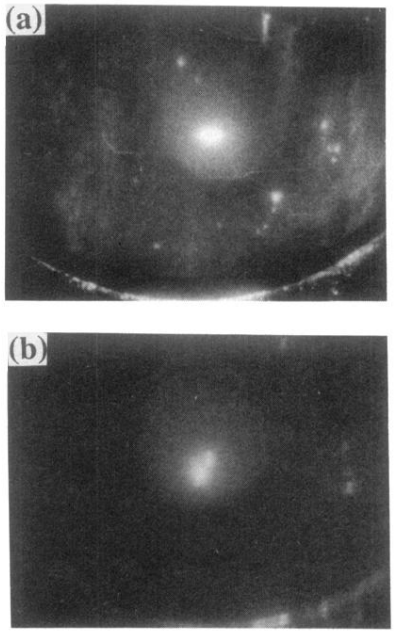


FIG. 4. Photographs of the phosphor screen during laser irradiation of (a) a polished MgO crystal (exposure time, 5 min) and (b) an oxygen deficient MgO thin film (exposure time, 1 min).